$[TlOTeF_5(mes)_2]_2$ and $[Tl(mes)_2^+][B(OTeF_5)_4^-]$ are in harmony with the molecular structures for these compounds. There are mutually exclusive IR and Raman ν(TeO) bands for $[TlOTeF_5(mes)_2]_2$, consistent with the nearly centrosymmetric structure of this dimer. The average ν(TeO) value of 823 cm^{-1} is between the low value for $HOTeF_5$ (733 cm^{-1}) and the high value for $[N(n\text{-}Bu)_4^+][OTeF_5^-]$ (867 cm^{-1}) and correlates well with the Te–O distances and δ_A for this compound (Table VIII). The compound $TlOTeF_5$ also exhibits mutually exclusive IR and Raman ν(TeO) bands. While little is known about the structure of this compound, the vibrational data indicate that it probably contains bridging $OTeF_5$ groups in the solid state.

A comparison of structural and spectroscopic data for the $B(OTeF_5)_4^-$ anion and for $B(OTeF_5)_3$[11,23] shows the expected trends. For example, the strong B–O bonds in $B(OTeF_5)_3$, with some degree of p–p π character, are consistent with weaker and longer Te–O bonds than found in the $B(OTeF_5)_4^-$ anion. The bands at 797 and 715 cm^{-1} for $[Tl(mes)_2^+][B(OTeF_5)_4^-]$ are tentatively assigned to the "A_1" and "T_2" stretching normal modes for the four Te–O oscillators in the $B(OTeF_5)_4^-$ anion. The symmetric stretch at 797 cm^{-1} is IR active (albeit weak) presumably because the $B(OTeF_5)_4^-$ anion does not possess strict T_d symmetry.

We have examined the ^{19}F NMR spectra of $[N(n\text{-}Bu)_4^+][B(OTeF_5)_4^-]$ and $[Tl(mes)_2^+][B(OTeF_5)_4^-]$ in dichloromethane at two different concentrations (see Experimental Section). There is a very slight cation dependence on δ_A for the $B(OTeF_5)_4^-$ anion and a smaller concentration dependence. These data demonstrate that some degree of ion pairing, whether specific or nonspecific, occurs for salts of $B(OTeF_5)_4^-$ in dichloromethane solution. Differences in cation–fluorine interactions for $[N(n\text{-}Bu)_4^+][B(OTeF_5)_4^-]$ and $[Tl(mes)_2^+][B(OTeF_5)_4^-]$ in the solid state could potentially be probed by Raman spectroscopy, since $OTeF_5$ compounds generally exhibit strong, sharp ν(TeF) bands.[22] The positions of these bands are sensitive to the environment of the $OTeF_5$ group(s).[22] However, both $B(OTeF_5)_4^-$ salts undergo photoinduced decomposition in the Raman spectrometer laser beam.

Conclusions. The compound $[Tl(mes)_2^+][B(OTeF_5)_4^-]$ has been prepared and fully characterized. Structural and spectroscopic data show that the $B(OTeF_5)_4^-$ anion is extremely weakly coordinated to $Tl(mes)_2^+$ in the solid state and in solution. This compound has already proven to be a useful reagent for introducing the $B(OTeF_5)_4^-$ anion by means of metathetical reactions of $[Tl(mes)_2^+][B(OTeF_5)_4^-]$ with metal and non-metal chlorides.[29] We intend to prepare a variety of salts of this anion with coordinatively unsaturated cations such as $Fe(porphyrin)^+$ and SiR_3^+. While there may be no such thing as a noncoordinating anion in condensed media, we propose that the $B(OTeF_5)_4^-$ anion is an excellent candidate for the least coordinating anion.

Acknowledgment. This research was supported by a grant from the National Science Foundation (CHE-8419719). We thank Professors J. R. Norton and A. T. Tu for the use of their IR and Raman spectrometers, respectively, and J. H. Reibenspies, P. K. Miller, and S. Zheng for experimental assistance. The Nicolet R3m/E diffractometer and computing system were purchased with a grant from the National Science Foundation (CHE-8103011).

Supplementary Material Available: Listings of anisotropic thermal parameters for all non-hydrogen atoms (Table S-I), hydrogen atom positions and isotropic thermal parameters (Table S-II), and C–C distances and C–C–C angles (Table S-III) for $[TlOTeF_5(mes)_2]_2 \cdot mes$ and listings of anisotropic thermal parameters for all non-hydrogen atoms (Table S-V) and C–C distances and C–C–C angles (Table S-VI) for $[Tl(mes)_2^+][B(OTeF_5)_4^-]$ (12 pages); listings of observed and calculated structure factors for both compounds (Tables S-IV and S-VII) (63 pages). Ordering information is given on any masthead page.

(29) Strauss, S. H.; Noirot, M. D., unpublished observations, 1986.

Contribution from the Department of Inorganic Chemistry, University of Melbourne, Parkville, Victoria 3052, Australia

Controlled Hydrolysis of the Hexafluorides of Molybdenum, Tungsten, and Rhenium: Structure of Oxonium (μ-Fluoro)bis(tetrafluorooxotungstate(VI))

Bernard F. Hoskins,* Anthony Linden, and Thomas A. O'Donnell*

Received September 12, 1986

The controlled hydrolysis reactions of the hexafluorides of molybdenum, tungsten, and rhenium in anhydrous hydrogen fluoride are reported. Vibrational spectra indicate that the hydrolysis of MoF_6 yields solely $MoOF_4$, as previously believed. Hydrolysis of ReF_6 yields a mixture of $ReOF_4$ and $H_3O^+Re_2O_2F_9^-$, while WF_6 hydrolyzes to give only $H_3O^+W_2O_2F_9^-$, even with excess WF_6. These reactions suggest that WOF_4 is a stronger Lewis acid than $MoOF_4$. $H_3O^+W_2O_2F_9^-$ crystallizes in the monoclinc space group $P2/n$ (a nonstandard setting of $P2/c$, No. 13). At 293 K, a = 14.818 (3) Å, b = 5.198 (1) Å, c = 5.576 (1) Å, β = 94.41 (1)°, V = 428.2 Å^3, and Z = 2. Refinement converged with R = 0.090, and R_w = 0.098 for 784 independent observed X-ray diffraction reflections. The structure consists of discrete ions with a fluorine-bridged $W_2O_2F_9^-$ anion. The angle at the bridge is 144 (2)° with the bridging W–F distance being 2.13 (1) Å. The average terminal W—F distance is 1.86 (2) Å, and W=O, being trans to the bridge, is 1.57 (3) Å. The fluorine and oxygen atoms are approximately hexagonally close packed.

Introduction

Some controlled hydrolysis reactions of several transition-metal hexafluorides in anhydrous hydrogen fluoride have been reported previously.[1-4] The products obtained were classified according to the electron affinities of each hexafluoride. The hexafluorides of Ir, Pt, and Ru have high electron affinity and oxidize water to form oxonium salts of the type $H_3O^+MF_6^-$ or $(H_3O^+)_2MF_6^{2-}$, while the low electron affinity hexafluorides of Mo, Re, Os, U and Np undergo fluorine substitution to form the metal oxide tetrafluorides. The latter reaction has provided a useful alternative to the thermal synthesis methods[5] often used to prepare some of these oxide tetrafluorides. The controlled hydrolysis of WF_6 has been found to give a product different from those described above. On the basis of vibrational spectra and elemental analyses, the

(1) Selig, H.; Sunder, W. A.; Disalvo, F. A.; Falconer, W. E. *J. Fluorine Chem.* **1978**, *11*, 39.
(2) Selig, H.; Sunder, W. A.; Schilling, F. C.; Falconer, W. E. *J. Fluorine Chem.* **1978**, *11*, 629.
(3) Wilson, P. W. *J. Chem. Soc., Chem. Commun.* **1972**, 1241.
(4) Peacock, R. D.; Edelstein, N. *J. Inorg. Nucl. Chem.* **1976**, *38*, 771.
(5) Cady, G. H.; Hargreaves, G. B. *J. Chem. Soc.* **1961**, 1568.

0020-1669/87/1326-2223$01.50/0

product was originally reported as $H_3O^+WOF_5^-$,[2] but more recent studies have suggested that it is $H_3O^+W_2O_2F_9^-$.[6]

In a program of study of the relative Lewis acid strengths of the oxide tetrafluorides of tungsten, molybdenum, and rhenium in anhydrous HF, we have sought low-temperature syntheses for these compounds that can be carried out in situ in Kel-F or synthetic sapphire tubes. Therefore, we have investigated further the hydrolysis reactions of WF_6. Our recent Raman spectroscopic and conductometric studies[7] in anhydrous HF give strong evidence that the anionic species generated in solution is $W_2O_2F_9^-$. In this paper we report both the isolation from HF solution of the crystalline compound $H_3O^+W_2O_2F_9^-$ and the determination of its crystal structure. Investigations of the controlled hydrolysis of MoF_6 and ReF_6 have also been carried out. The results confirm $MoOF_4$ as the hydrolysis product of MoF_6 but suggest that, in HF solution, ReF_6 hydrolyzes to a mixture of $ReOF_4$ and $H_3O^+Re_2O_2F_9^-$.

Experimental Section

Apparatus and Materials. Volatile compounds were manipulated in a stainless-steel vacuum line, which was equipped with stainless-steel 1KS4 Kel-F-tipped Whitey valves. The vacuum line was well passivated with ClF_3 before use. Pressures from vacuum to 5 atm were measured by using Bourdon gauges, with a thermocouple gauge being used in the range 0–500 mTorr. Nonvolatile solid samples were manipulated in a dry-atmosphere glovebox. Reactions were carried out in Kel-F tubes or sapphire tubes fitted with Kel-F valves.[8]

Hydrogen fluoride (Matheson, 99.5%) was purified by four trap-to-trap distillations as described previously.[9] The hexafluorides of molybdenum, tungsten, and rhenium (Ozark Mahoning, 98%) were used after a single distillation from a source cylinder.

Raman spectra were recorded on a Spex Ramalog instrument using the 514.5-nm exciting line of an Ar^+ laser. Solid samples were contained in glass capillaries, while a Kel-F cell fitted with three sapphire windows, based on a design for UV–visible cells,[9] was used for solution measurements. Infrared spectra were recorded on a Jasco A-302 spectrophotometer. Spectra of solids were obtained by using dry powders pressed between AgCl plates. Kel-F grease on the edges of the plates was used to minimize hydrolysis of the samples.

Elemental analyses were carried out on the compound $H_3O^+W_2O_2F_9^-$. After base hydrolysis of a sample, the tungsten in solution, buffered with borate, was determined by potentiometric titration with $AgNO_3$.[10] Fluoride was determined by using a standard procedure involving a fluoride ion selective electrode.[11]

Hydrolysis Reactions of MoF_6 and WF_6. A controlled amount of water was generated in the reaction vessel by the reaction between anhydrous HF and boric acid. This reaction was designed to produce BF_3 and a controlled amount of water, that amount being somewhat less than that required for a stoichiometric reaction with the hexafluoride MF_6 to yield MOF_4. In a typical reaction, recrystallized boric acid (0.20 g) was dissolved in HF (5 cm^3), after which the generated BF_3 was distilled off at −78 °C. A substantial excess of the appropriate hexafluoride was condensed into the tube and the mixture allowed to warm to room temperature. The excess hexafluoride used was sufficient to exceed its solubility in HF, so that at room temperature two liquid layers were visible. After several hours all volatile material was removed under vacuum at ambient temperature, leaving a white solid. For the hydrolysis of MoF_6, the solid (1.85 g; weight calculated for $MoOF_4$ from 0.20 g of H_3BO_3 is 1.82 g) was identified by Raman spectroscopy as $MoOF_4$.[12,13] The hydrolysis product of WF_6 (1.78 g; weight calculated for $H_3O^+W_2O_2F_9^-$ from 0.20 g of H_3BO_3 is 1.93 g) was identified by vibrational spectroscopy as consisting of predominantly $H_3O^+W_2O_2F_9^-$. Anal. Calcd for $H_3O^+W_2O_2F_9^-$: W, 62.3; F, 29.0. Found: W, 60.8; F, 29.2.

Hydrolysis of ReF_6. This reaction was carried out by using a procedure similar to that described above except that a substoichiometric amount of distilled water was pipetted directly into the empty Kel-F tube rather than generating the water from boric acid. The water was dissolved in HF, and a 10% excess of ReF_6 was condensed onto the solution. A deep blue color developed, which suggested the formation of $ReOF_4$. A pure solid sample could not be isolated as decomposition to olive green and black residues occurred when the HF was distilled from the solution. A Raman spectrum of the blue solution indicated a mixture of $ReOF_4$[14] and $Re_2O_2F_9^-$,[15] in which the latter was probably present as H_3O^+-$Re_2O_2F_9^-$.

Table I. Crystal Data for $H_3O^+W_2O_2F_9^-$

composition	$H_3F_9O_3W_2$
fw	589.8
cryst class	monoclinic
space group	$P2/n$ (nonstandard setting of $P2/c$, C_{2h}^4, No. 13)
a, Å	14.818 (3)
b, Å	5.198 (2)
c, Å	5.576 (1)
β, deg	94.41 (1)
V, Å^3	428.21
Z	2
D_{calcd}, Mg m^{-3}	4.57
$F(000)$	512
radiation	Mo Kα (graphite monochromated)
λ, Å	0.71069
μ, cm^{-1}	275.7
cryst dimens, mm	0.42 × 0.33 × 0.42
transmissn factors	max 0.0510; min 0.0042
scan range, deg	$1 \leq 2\theta \leq 55$
reflcn forms recorded	$\pm h,\pm k,\pm l$ for $2\theta \leq 50°$ $+h,\pm k,\pm l$ for $2\theta > 50°$
no. of reflcns measd	4084
no. of unique reflcns	977 (784 obsd)
criterion of observability	$I \geq 2\sigma(I)$
no. of params refined	36
R_{amal}	0.118
residuals	$R = 0.090$; $R_w = 0.098$

X-ray Data Collection. Crystals of $H_3O^+W_2O_2F_9^-$ were grown by the slow concentration of solutions of the adduct in anhydrous HF in sapphire reaction tubes. Crystal growth was hindered by the high solubility of the adduct in HF. Large amounts of solid usually precipitated rapidly from a saturated solution. This resulted in clusters of poorly defined crystals, which proved difficult to separate. After repeated recrystallizations, a few irregularly shaped colorless crystals were isolated, mostly with strongly adhering crystallites. The excess solution was decanted and the tube was gently evacuated and filled with dry nitrogen. The crystals were transferred into Lindemann glass capillaries in the dry-atmosphere glovebox. Preliminary oscillation and equiinclination Weissenberg photographs indicated that the crystals were generally of poor quality, with the presence of several misaligned fragments. The very high reactivity of the crystals was evidenced by rapid decomposition with time and/or irradiation. The crystal used for data collection was one that exhibited minimal disorder on a preliminary oscillation photograph.

The selected crystal was mounted on an Enraf Nonius CAD-4F four-circle diffractomer. The procedures for obtaining accurate unit cell parameters and their estimated standard deviations, together with an accurate orientation matrix, have been described previously.[16] The crystal data and data collection parameters are summarized in Table I. Intensity data were collected at room temperature (293 K) by using the ω–2θ scan technique and graphite-monochromated Mo Kα radiation. In order to minimize the decomposition of the crystal in the X-ray beam, the maximum scan time used for each reflection was 30 s; however, the crystal still deteriorated to approximately 60% of its original scattering power during the data collection. This decomposition was cause for serious concern, but there was little choice because of the difficulty of preparing and isolating several crystals that did not exhibit too many disordered fragments. The density of the crystal was not measured, but the assumption that two molecules would occupy each unit cell leads to a volume per light atom of 17.8 Å^3, consistent with the corresponding volume of 18–20 Å^3 found for close packing of oxygen and fluorine atoms in similar compounds.[17–19]

(6) Wilson, W. W.; Christe, K. O. *Inorg. Chem.* **1981**, *20*, 4139.
(7) Canale, G. Research Report, University of Melbourne, 1982.
(8) Canterford, J. H.; O'Donnell, T. A. In *Technique of Inorganic Chemistry*; Jonassen, H. B., Weissberger, A., Eds.; Interscience: New York, 1968; Vol. VII, p 273.
(9) Barraclough, C. G.; Cockman, R. W.; O'Donnell, T. A. *Inorg. Chem.* **1977**, 16, 673.
(10) Irvine, I. Ph.D. Thesis, University of Melbourne, 1975.
(11) *Annu. Book ASTM Stand.* **1979**, *31*, 373, D1179.
(12) Alexander, L. E.; Beattie, I. R.; Bukovsky, A.; Jones, P. J.; Marsden, C. J.; Van Schalkwyk, G. J. *J. Chem. Soc., Dalton Trans.* **1974**, 81.
(13) Bougon, R.; Bui Huy, T.; Charpin, P. *Inorg. Chem.* **1975**, *14*, 1822.
(14) Paine, R. T.; Treuil, K. L.; Stafford, F. E. *Spectrochim. Acta, Part A* **1973**, *29A*, 1891.
(15) Rigoni, P. Research Report, University of Melbourne, 1984.
(16) Hoskins, B. F.; Linden, A.; Mulvaney, P. C.; O'Donnell, T. A. *Inorg. Chim. Acta* **1984**, *88*, 217.
(17) Zachariasen, W. H. *Acta Crystallogr.* **1949**, *2*, 390.
(18) Edwards, A. J.; Jones, G. R. *J. Chem. Soc. A* **1968**, 2511.

Table II. Fractional Atomic Positions for $H_3O^+W_2O_2F_9^-$ with Estimated Standard Deviations in Parentheses

atom	x	y	z
W	0.1132 (1)	0.7348 (2)	0.7507 (2)
F(1)	0.25	0.861 (6)	0.75
F(2)	0.163 (1)	0.463 (4)	0.588 (4)
F(3)	0.160 (2)	0.586 (4)	1.035 (4)
F(4)	0.103 (2)	1.042 (4)	0.926 (4)
F(5)	0.103 (2)	0.917 (4)	0.466 (4)
O(1)	0.012 (2)	0.648 (5)	0.752 (4)
O(2)	0.25	0.179 (7)	0.25

Structure Solution and Refinement. Structure determination and refinement were performed by using the SHELX-76 program system[20] and the University of Melbourne's Cyber 170-730 and Vax 11/780 computer systems. The scattering factors used for oxygen and fluorine were those collected by Sheldrick,[20] while the atomic scattering factor for tungsten was obtained from ref 21a. These values were corrected for the real and imaginary parts of anomalous dispersion.[21b] The data were corrected for Lorentz and polarization effects, crystal decomposition, and absorption.[20,21c] Absorption corrections, which were numerically evaluated by Gaussian integration,[20] were difficult to apply accurately due to the high absorption coefficient of the crystal coupled with the difficulty experienced in describing the morphology of the crystal. All crystals examined possessed irregular faces, which were caused by the adherance of the crystals to the surface of the sapphire tube used for their growth. Difficulties were also encountered in the interpretation of systematic absences in the photographic and diffraction data. The absences suggested the condition $h0l$, $h + l = 2n + 1$, which is consistent with the space groups Pn and $P2/n$. There were, however, several of these reflections that were weakly observable. These reflections probably arose from satellite crystals, but initially it was necessary to consider additionally the space groups $P1$, $P\bar{1}$, $P2$, Pm, and $P2/m$. The three-dimensional Patterson synthesis revealed vectors associated with the tungsten atoms that could only be rationalized in terms of the space groups $P2/n$, $P\bar{1}$, and $P1$.

Amalgamation of equivalent reflections in the space group $P2/n$ gave $R_{amal} = 0.118$[22] and approximately 70 inconsistent amalgamations were listed, which suggested that an attempt was being made to amalgamate nonequivalent reflections. A significantly lower value of $R_{amal} = 0.065$ and only seven inconsistencies were obtained when the data were amalgamated in the space group $P\bar{1}$. These results suggested that the structure possibly did not conform exactly to a monoclinic space group and that the cell dimensions were only fortuitously very close to those of a monoclinic cell.

The initial stages of refinement of the structure were therefore carried out in both of the space groups $P\bar{1}$ and $P2/n$. The positions of the tungsten atoms were determined from the Patterson map, and the oxygen and fluorine atoms were placed from subsequent difference-Fourier syntheses. The structure was refined by using a full-matrix least-squares technique.[23] Refinement of the atomic positions in the space group $P2/n$ with anisotropic thermal parameters for the tungsten atom, individual isotropic temperature factors for the light atoms, and unit weights, converged with $R = 0.10$. Analogous refinement in the space group $P\bar{1}$ yielded $R = 0.12$.

Refinement was continued in the space group $P2/n$, but the refinement of anisotropic thermal parameters was not successful for all light atoms so, for the final refinement cycles, anisotropic thermal parameters were used for the tungsten atom only. A weighting scheme was also employed where $w = 5.45[\sigma^2(F_o) + 0.0026F_o^2]^{-1}$ and an isotropic extinction coefficient, x, was included.[24] Refinement converged at a final $R = 0.090$ ($R_w = 0.098$) and $x = 0.0035$ (6) for 784 unique observed reflections ($I \geq 2\sigma(I)$). The maximum parameter shift in the final refinement cycle was 0.01σ, and the analysis of variance showed no systematic trends.

Table III. Intraionic Distances (Å) and Angles (deg) for $H_3O^+W_2O_2F_9^-$[a]

W-F(1)	2.13 (1)	F(1)···F(2)	2.57 (3)
W-F(2)	1.86 (2)	F(1)···F(3)	2.58 (3)
W-F(3)	1.85 (2)	F(1)···F(4)	2.64 (3)
W-F(4)	1.88 (2)	F(1)···F(5)	2.61 (2)
W-F(5)	1.84 (2)	F(2)···F(3)	2.58 (3)
W-O(1)	1.57 (3)	F(2)···F(5)	2.59 (3)
O(1)···F(2)	2.66 (3)	F(3)···F(4)	2.57 (3)
O(1)···F(3)	2.62 (3)	F(4)···F(5)	2.64 (3)
O(1)···F(4)	2.60 (3)	F(2)···F(2)^I	3.03 (3)
O(1)···F(5)	2.58 (3)	F(2)···F(3)^I	2.84 (3)
W-F(1)-W^I	144 (2)	O(1)-W-F(1)	179 (1)
O(1)-W-F(2)	101 (1)	O(1)-W-F(3)	100 (1)
O(1)-W-F(4)	97 (1)	O(1)-W-F(5)	98 (1)
F(2)-W-F(3)	88 (1)	F(2)-W-F(4)	161 (1)
F(2)-W-F(5)	89 (1)	F(2)-W-F(1)	80 (1)
F(3)-W-F(4)	87 (1)	F(3)-W-F(5)	162 (1)
F(3)-W-F(1)	81 (1)	F(4)-W-F(5)	90 (1)
F(4)-W-F(1)	82 (1)	F(5)-W-F(1)	82 (1)

[a] Superscript I refers to the following transformation: $^1/_2 - x$, y, $1\,^1/_2 - z$.

Table IV. Vibrational Stretching Frequencies for the M=O Bond of the Oxide Tetrafluorides and Related Anions

	ν(M=O), cm^{-1}			
metal (M)	MOF_4	$M_2O_2F_9^-$	MOF_5^-	ref
Mo	1048	1020–1026	985–1011	12, 13
W	1055	1038–1042	1001	12, 13
Re	1070–1072		1002–1012	14, 27, 28

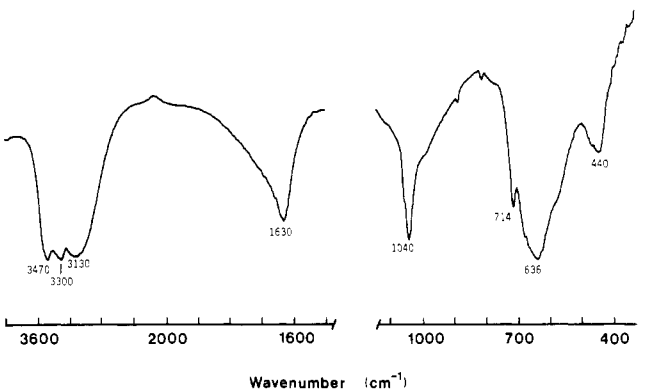

Figure 1. Infrared spectrum of $H_3O^+W_2O_2F_9^-$.

Since all parameters had converged satisfactorily and the structure was well defined with acceptable thermal parameters, the relatively high R values were attributed to the decomposition of the crystal. No alternative model could be found nor evidence to suggest superlattice effects.[25] The highest residual peaks in the final difference map were 9 e Å^{-3} and were within 1.0 Å of the tungsten atom. When the magnitudes of these residual peaks were considered in the context of the electron density value calculated for the tungsten atom, they corresponded to 1.9 electrons. No attempt was made to locate the hydrogen atoms of the cation, because of these residual peaks.

The parallel refinement using the space group $P\bar{1}$ yielded atomic positions that were clearly related by a 2-fold axis passing through the bridging fluorine atom of the anion and corresponded almost exactly with the atomic positions obtained by using the space group $P2/n$. Strong correlation between parameters also suggested a 2-fold relationship. No improvement in the refinement was obtained by using the space group $P\bar{1}$, and the residual peaks in the final difference map were 13 e Å^{-3} (corresponding to 3.0 electrons). It was therefore considered that the structure could be best described in the space group $P2/n$, despite the high R_{amal} and inconsistencies obtained for amalgamation of the data, which were probably due to the problems outlined above. Similar difficulties with high residuals and poor amalgamations have been attributed

(19) Edwards, A. J.; Sills, R. J. C. *J. Chem. Soc., Dalton Trans.* **1974**, 1726.
(20) Sheldrick, G. M. "SHELX-76, Program for Crystal Structure Determination"; University of Cambridge: Cambridge, U.K., 1976.
(21) *International Tables for X-ray Crystallography*; Kynoch: Birmingham, England, 1974; Vol. IV: (a) p 99; (b) p 149; (c) p 61.
(22) $R_{amal} = (\sum\{N\sum[w(F_{mean} - |F_o|)^2]\}/\sum[(N-1)\sum(w|F_o|^2)])^{1/2}$ where the inner summations are over N equivalent reflections averaged to give F_{mean}, the outer summations are over all unique reflections, and the weight, w, is taken as $[\sigma(F_o)]^{-2}$.
(23) The function minimized was $\sum w(|F_o| - |F_c|)^2$, where w was the weight applied to each reflection. The unweighted and weighted residuals were defined as $R = \sum(||F_o| - |F_c||)/\sum|F_o|$ and $R_w = \sum[w^{1/2}(||F_o| - |F_c||)]/\sum(w^{1/2}|F_o|)$ respectively.
(24) The form of the correction for secondary extinction is $|F_{cor}| = |F_o|[1 - (0.0001F_c^2/(\sin\theta)]$.
(25) Ibers, J. A. In *Critical Evaluation of Physical and Structural Information*; Lide, D. R., Jr., Paul, M. A., Eds.; National Academy of Sciences: Washington, DC, 1974; p 186.

previously[26] to severe crystal decomposition and the presence of crystallites.

The final fractional atomic coordinates are listed in Table II. The intraionic distances and angles are given in Table III.

Results and Discussion

Vibrational Spectra. The frequencies of the metal–oxygen stretching vibrations exhibited by the oxide tetrafluorides of Mo, W, and Re and their related anions, MOF_5^- and $M_2O_2F_9^-$, have been shown to be characteristic of the species present. For a given metal, values of ν(M=O) for the molecular and each of the anionic species are sufficiently distinct to enable vibrational spectra to be used diagnostically to determine which of these species is present in a sample. Table IV lists some of the expected values for ν(M=O). The trend of M=O stretching frequencies reflects the effect on the metal–oxygen bond strength of the presence of a fluorine atom trans to oxygen. ν(M=O) increases when the trans terminal fluorine of MOF_5^- is replaced by a weaker M—F—M fluorine bridge and increases further when there is no atom trans to the oxygen, as in MOF_4.

The infrared spectrum of the hydrolysis product of WF_6 is shown in Figure 1. ν(W=O) at 1040 cm^{-1} clearly indicates the presence of the anion $W_2O_2F_9^-$. The other bands in the 400–1200-cm^{-1} region of the spectrum are also in precise agreement with those observed by Bougon et al.[13] for the anion of the salt $NO^+W_2O_2F_9^-$. The broad bands observed in the 3100–3500-cm^{-1} region and at 1630 cm^{-1} are characteristic of H_3O^+.[29] Raman spectra of the solid adduct, and its solution in anhydrous HF, exhibited major bands at 1042, 718, and 318 cm^{-1}, again characteristic of the anion $W_2O_2F_9^-$. These results, particularly the W=O stretching frequencies, show that neither WOF_4 nor the anion WOF_5^- is present in the samples and support the formulation of the hydrolysis product as $H_3O^+W_2O_2F_9^-$.

The Raman spectrum of an HF solution of the hydrolysis product of MoF_6 showed the Mo=O stretching vibration at 1042 cm^{-1}, which is indicative of the presence of $MoOF_4$. No indication of $Mo_2O_2F_9^-$ or $MoOF_5^-$ could be detected in the spectrum, which was very similar to that reported previously for $MoOF_4$.[12,13] A Raman spectrum of the solid isolated from the solution was also consistent with that of $MoOF_4$.

A Raman spectrum of an HF solution of the hydrolysis product of ReF_6 contained two bands in the Re=O stretching region. A sharp band at 1072 cm^{-1} was consistent with ν(Re=O) of $ReOF_4$.[14] A second band, approximately twice as intense as the 1072-cm^{-1} band, was observed at 1057 cm^{-1}. Although a value for ν(Re=O) of $Re_2O_2F_9^-$ has not been reported previously, the trends of M=O stretching frequencies indicated in Table IV for the molybdenum and tungsten species suggest that the band at 1057 cm^{-1} would be consistent with $Re_2O_2F_9^-$. ν(Re=O) in the equivalent cation, $Re_2O_2F_9^+$, has been reported at 1059 cm^{-1}.[30] It could therefore be expected that ν(Re=O) for the anion should be similar. Unfortunately the sensitivity of the rhenium solutions to decomposition did not permit the isolation and further characterization of the hydrolysis products. The spectrum suggests that the major products of hydrolysis of ReF_6 are $ReOF_4$ and $Re_2O_2F_9^-$, produced in the approximate ratio 1:2. Bougon et al.[13] have shown that, in anhydrous HF, the species MOF_4 and $M_2O_2F_9^-$ (M = Mo, W) are in equilibrium and that the equilibrium lies strongly in favour of MOF_4. It is therefore unlikely that the significant concentration of $Re_2O_2F_9^-$ observed is the result of a similar equilibrium with $ReOF_4$. Furthermore, Raman spectra have indicated that HF solutions of pure $ReOF_4$, which had been prepared by a nonhydrolysis pathway,[31] contained only very small amounts of $Re_2O_2F_9^-$ after equilibrium was established. Thus the $Re_2O_2F_9^-$ must have been generated as part of the hydrolysis reaction, and by analogy with the hydrolysis product of WF_6, the $Re_2O_2F_9^-$ is probably present as $H_3O^+Re_2O_2F_9^-$.

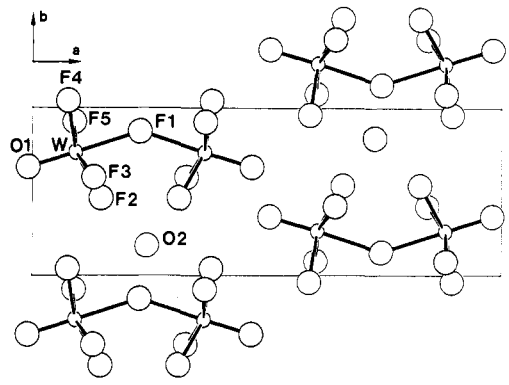

Figure 2. Projection of the structure of $H_3O^+W_2O_2F_9^-$ onto the plane (001).

Structure of $H_3O^+W_2O_2F_9^-$. With the crystal decomposition and difficulty in assigning the space group in mind, the results obtained here should be considered as somewhat tentative. However, we believe that there is little doubt about the overall features of the structure. A projection of the $H_3O^+W_2O_2F_9^-$ structure is shown in Figure 2. The anion consists of two WOF_4 units bridged together by a fluorine atom, this bridge being trans to the tungsten–oxygen bonds. This is consistent with the proposed formula, $W_2O_2F_9^-$, deduced from the Raman spectra and chemical analysis. Although oxygen and fluorine atoms can be difficult to distinguish in X-ray diffraction data, these atoms were assigned on the basis of their bond lengths with tungsten. For the similar compounds, MOF_4 (M = Mo, W, Re),[18,32,33] the average terminal M—F bond lengths are 1.84 Å while the average terminal M=O distances are 1.64 Å. In $H_3O^+W_2O_2F_9^-$, the average W—F terminal bond length is 1.86 (4) Å while the terminal bonds trans to the bridge are 1.57 (3) Å and can therefore be assigned reasonably as W=O bonds. On the basis of the Raman spectra, it is unlikely that the bridging atom is oxygen.

A proposal has been made by Cotton[34] that there is a general tendency for bonds trans to electron-withdrawing M=O multiple bonds to be weakened and therefore lengthened. This effect is exemplified by the structure of $MoOF_4$, in which $MoOF_4$ units are linked into chains by cis fluorine bridging. By necessity, the bridging fluorine is trans to the oxygen atom of one molybdenum but trans to a terminal fluorine atom on the other molybdenum.[33] The asymmetric bridge, with an F—Mo distance of 2.27 Å trans to Mo=O and 1.96 Å trans to terminal Mo—F, clearly demonstrates the lengthening effect on a bridging fluorine bond of an electron-withdrawing terminal oxygen atom trans to that bridge. The effect can be demonstrated by comparing the bond lengths in $W_2O_2F_9^-$ with those in the fluorine-bridged dimeric anion in $I_2^+Sb_2F_{11}^-$.[35] In $W_2O_2F_9^-$ the bridging F—W distance (trans to the short W=O bond of 1.57 Å) is 2.13 Å, while the average length to the terminal F—W bonds is 1.86 Å. In $Sb_2F_{11}^-$ the bridging F–Sb distance trans to a terminal F–Sb is 2.00 Å, with the average of the terminal F–Sb distances again being 1.86 Å. $I_2^+Sb_2F_{11}^-$ has been chosen deliberately for purposes of comparison because in that compound interaction of the cation I_2^+ with the anion $Sb_2F_{11}^-$ is minimal as is the case for $H_3O^+W_2O_2F_9^-$ as discussed below. The small interaction results in a symmetrical dimeric anion; i.e., bridging fluorine-to-metal distances are the same for both metal atoms in each of the anions. Gillespie and colleagues[35] point out that as the cation becomes a progessively stronger Lewis acid; e.g., in progressing from I_2^+ through XeF_3^+

(26) Holloway, J. H.; Kaucic, V.; Martin-Rovet, D.; Russell, D. R.; Schrobilgen, G. J.; Selig, H. *Inorg. Chem.* **1985**, *24*, 678.
(27) Kuhlmann, W.; Sawodny, W. *J. Fluorine Chem.* **1977**, *9*, 341.
(28) Holloway, J. H.; Raynor, J. B. *J. Chem. Soc., Dalton Trans.* **1975**, 737.
(29) Christe, K. O.; Schack, C. J.; Wilson, R. D. *Inorg. Chem.* **1975**, *14*, 2224.
(30) Schrobilgen, G. J.; Holloway, J. H.; Russell, D. R. *J. Chem. Soc., Dalton Trans.* **1984**, 1411.
(31) Burns, R. C.; O'Donnell, T. A.; Waugh, A. B. *J. Fluorine Chem.* **1978**, *12*, 505.
(32) Edwards, A. J.; Jones, G. R. *J. Chem. Soc. A* **1968**, 2075.
(33) Edwards, A. J.; Steventon, B. R. *J. Chem.Soc. A* **1968**, 2503.
(34) Cotton, F. A.; Morehouse, S. M.; Wood, J. S. *Inorg. Chem.* **1964**, *3*, 1603.
(35) Davies, C. G.; Gillespie, R. J.; Ireland, P. R., Sowa, J. M. *Can. J. Chem.* **1974**, *52*, 2048.

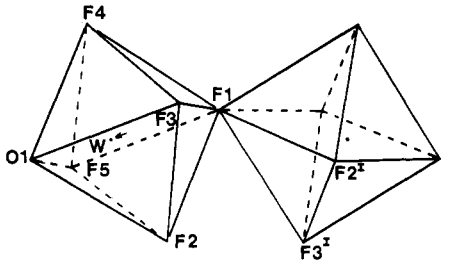

Figure 3. Corner-shared octahedra formed by the light atoms in the anion of $H_3O^+W_2O_2F_9^-$. The displacement of the tungsten atom toward the oxygen atom is arrowed.

and XeF^+ to BrF_4^+ in compounds for which the counteranion is $Sb_2F_{11}^-$, covalent interaction through fluorine bridging between the formal cation and the formal anion becomes steadily greater and this leads to a progressive lowering of symmetry in the Sb–F–Sb bridging system within the $Sb_2F_{11}^-$ anion. There are many similar examples in structures of compounds that contain both a fluoro cation and a fluoro anion in which some degree of fluorine bridging between cation and anion leads to reduced symmetry in a dimeric fluorine-bridged anion.

The arrangement of light atoms in the $W_2O_2F_9^-$ anion forms two corner-shared octahedra related by a 2-fold axis, as shown in Figure 3. Although there is considerable variation in the bond lengths around the tungsten atoms, the octahedra formed by the light atoms are relatively undistorted, as shown by Table III. The average light atom to light atom distance is 2.60 Å with all intraionic contacts falling within the range 2.57–2.66 Å. Calculations of the least-squares planes of the light atoms making up the octahedra and the deviations of all atoms from these planes show that the maximum displacement of any atom from its plane is 0.026 Å. The tungsten atom lies 0.29 Å out of the plane defined by F(2), F(3), F(4), and F(5), being distorted along the diagonal of the octahedron toward the oxygen atom. This gives rise to the short W=O bond and the long bridging W—F bond.

The bond angle about the bridging fluorine atom of the anion can be related to the type of close packing adopted by the light atoms in the structure. Edwards[18] has shown that for the idealized case of a hexagonally close packed structure with metal atoms in octahedral sites, the angle at the bridge atom would be 132°, whereas for cubic close packing this angle would be 180°. For example, the structure of WOF_4[32] shows approximate cubic close packing of light atoms and has a bridging angle of 173°. In contrast, the structure of $ReOF_4$, in which the light atoms are approximately hexagonally close packed, shows a bridging angle of 139°.[18] The bond angle at the bridging fluorine atom of the $W_2O_2F_9^-$ anion, which is situated on a 2-fold axis, is 144°. While this angle is significantly larger than the idealized angle for hexagonal close packing, it indicates that the light atoms are in an arrangement which is not distorted too far from this type of packing. The interionic contact distances (supplementary data) are all within the range 2.73–3.24 Å, which is also consistent with close packing of the light atoms.

Difference maps revealed that the cation contains only a single non-hydrogen atom, which suggests either H_2F^+ or H_3O^+ as the cation. The quality of the data did not permit the location of the hydrogen atoms, and the cation was assigned as H_3O^+ on the basis of chemical analysis and the spectroscopic data. Figure 4 shows the coordination of the cation. Each of the four anions surrounding the cation, approximately in the (100) plane, provides two contacts to the cation through fluorine atoms. The eight contacts form a severely distorted cube of fluorine atoms around the cationic oxygen atom. There are no near contacts between the cation and an oxygen atom of the nearest anion along the [100] direction. The F···O(2) contact distances are within the range 2.73–2.91 Å and are consistent with the distances between these atoms in other hydrogen-bonded compounds.[36] This suggests that there is some

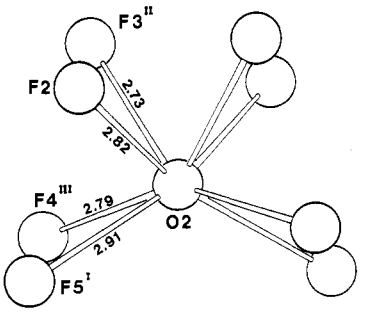

Figure 4. Coordination environment of the cation in $H_3O^+W_2O_2F_9^-$.

Table V. Composition of the Possible Adducts from the Hydrolysis of WF_6

	anal.	
	% W	% F
Calculated		
WOF_4	66.6	27.5
$H_2F^+WOF_5^-$	58.2	36.1
$H_3O^+WOF_5^-$	58.6	30.3
$H_2F^+W_2O_2F_9^-$	62.1	32.1
$H_3O^+W_2O_2F_9^-$	62.3	29.0
Found		
this work	60.8	29.2
Selig et al.[a]	59.0	29.2

[a] Reference 2.

interaction, due to weak hydrogen bonding, between the H_3O^+ cation and the fluorine atoms of the $W_2O_2F_9^-$ anion. The degree of interaction, however, is not sufficiently strong to cause significant lengthening of the W–F terminal bonds. It also appears that every terminal fluorine atom is involved in a contact with one of the three hydrogen atoms of the cation, a feature which would also decrease the extent of each interaction. The weakness of the hydrogen bonding suggests that it is appropriate to refer to $H_3O^+W_2O_2F_9^-$ as an ionic adduct. The hydrogen bonding in this adduct is weaker than in the related compound, $H_3O^+TiF_5^-$,[37] which has also been described as ionic. In that compound the F···O distances between the anion and cation were in the range 2.50–2.55 Å, which demonstrated significant hydrogen bonding. In addition, there were only three close contacts between the cation and the anion, which indicated that each hydrogen atom only interacted with one fluorine atom.

General Discussion. Selig et al.[2] have reported that the hexafluorides of Mo, Re, and Os, each with low electron affinity, undergo controlled hydrolysis to yield the metal oxide tetrafluoride. This has been confirmed in the case of MoF_6; however, we have shown that the hydrolysis of ReF_6 gives a mixture of $ReOF_4$ and $H_3O^+Re_2O_2F_9^-$. This can be explained in terms of the stronger Lewis acidity of $ReOF_4$, which favours retention of an ionic adduct in preference to the complete reaction of H_3O^+ with excess ReF_6 to yield $ReOF_4$ alone. For the weaker Lewis acid $MoOF_4$, the $Mo_2O_2F_9^-$ anion more readily loses fluoride, thereby generating $MoOF_4$ and freeing H_3O^+ to react further with MoF_6. Thus, $MoOF_4$ is the only product observed. A similar argument can be applied to the hydrolysis of WF_6, where the sole product, $H_3O^+W_2O_2F_9^-$, indicates that WOF_4 must be a stronger Lewis acid.

Selig et al.[2] have reported that the hydrolysis product of WF_6 is $H_3O^+WOF_5^-$. They proposed that their Raman spectrum of the adduct, which was almost identical with that obtained in this work, corresponded to a distorted WOF_5^- anion. While they noted that ν(W=O) was significantly different from that observed in $CsWOF_5$,[13] they also based their deductions on elemental analyses. As shown in Table V, all the possible hydrolysis products have quite similar compositions, so that it can be difficult to determine precisely which compound is present. It can be seen from this

(36) Hamilton, W. C.; Ibers, J. A. *Hydrogen Bonding in Solids*; Benjamin: New York, 1968.

(37) Cohen, S.; Selig, H.; Gut, R. *J. Fluorine Chem.* **1982**, *20*, 349.

work and Selig's analytical results[2] that the fluoride analyses were very close to the expected value for $H_3O^+W_2O_2F_9^-$ and that the tungsten analyses fell between the values predicted for $H_2O^+W_2O_2F_9^-$ and $H_3O^+WOF_5^-$.

Since infrared spectra and X-ray diffraction data cannot distinguish easily between H_2F^+ and H_3O^+, another possible hydrolysis product could be $H_2F^+W_2O_2F_9^-$; however, this was ruled out on the basis of the fluoride analysis. As mentioned earlier, the equilibrium between WOF_4 and $W_2O_2F_9^-$ in HF solution strongly favors WOF_4.[13] If $H_2F^+W_2O_2F_9^-$ or WOF_4 was being formed, the Raman spectrum of the HF solution should have shown significant amounts of WOF_4, which would be present as a result of the action of the equilibrium. The $W_2O_2F_9^-$, therefore, must be generated directly from the hydrolysis reaction and not indirectly via the initial formation and reequilibration of WOF_4. This can only occur if a cation is present that is not derived from the solvent. The product, $H_3O^+W_2O_2F_9^-$, suggested by the experimental evidence, is consistent with this requirement.

It has also been proposed[6] that, provided an excess of WF_6 is used, the hydrolysis of WF_6 will yield WOF_4 and that the products, $H_3O^+WOF_5^-$ or $H_3O^+W_2O_2F_9^-$, will only occur in the presence of excess water. The preparation of $H_3O^+W_2O_2F_9^-$ reported here has shown that even with a substantial excess of WF_6 and after several hours reaction time, the hydrolysis product is predominantly $H_3O^+W_2O_2F_9^-$. While the use of excess WF_6 might be expected to favor the formation of WOF_4 on the grounds of stoichiometry, the oxonium adduct is apparently quite stable in HF and is resistant to conversion to WOF_4 by further reaction between H_3O^+ and WF_6.

These results indicate that the controlled hydrolysis of WF_6 and ReF_6 in anhydrous HF is not a viable synthetic route to WOF_4 and $ReOF_4$ although $ReOF_4$ has been reported as the major reaction product when ReF_6 reacts with quartz or glass wool containing small amounts of H_2O or HF.[38] The hydrolysis of MoF_6 in anhydrous HF does, however, readily yield pure $MoOF_4$.

Acknowledgment. This work was supported in part by the Australian Research Grants Scheme. A.L. is grateful for the financial assistance provided by a Commonwealth Postgraduate Research Award.

Registry No. MoF_6, 7783-77-9; ReF_6, 10049-17-9; WF_6, 7783-82-6; HF, 7664-39-3; $MoOF_4$, 14459-59-7; $ReOF_4$, 17026-29-8; H_3O^+-$Re_2O_2F_9^-$, 108122-10-7; $H_3O^+W_2O_2F_9^-$, 108210-98-6.

Supplementary Material Available: Listings of thermal parameters, interionic contact distances less than 3.5 Å, and deviations from least-squares mean planes (3 pages); a listing of observed and calculated structure factors (2 pages). Ordering information is given on any current masthead page.

(38) Paine, R. T. *Inorg. Chem.* **1973**, *12*, 1457.

Contribution from Battelle, Pacific Northwest Laboratories, Richland, Washington 99352

Solubility of Amorphous Chromium(III)-Iron(III) Hydroxide Solid Solutions

Bruce M. Sass† and Dhanpat Rai*

Received December 31, 1986

Neutralization of acidic solutions containing Cr(III) and Fe(III) at room temperatures results in coprecipitation of these elements as an amorphous solid solution [$Cr_xFe_{1-x}(OH)_3$]. The solubilities of the $Cr_xFe_{1-x}(OH)_3$ precipitates prepared with different mole fractions (x) of $Cr(OH)_3$ (0.99, 0.89, 0.69, 0.49, 0.36, 0.15, 0.09, 0.01, 0.00) were determined in 0.01 M perchlorate solutions between pH 2 and 6 in an N_2 atmosphere. The Cr concentrations in 0.0018-μm filtrates at various times between 5 and 210 days, from initially undersaturated and oversaturated solutions, show that equilibrium was attained within about 7 days when $x < 0.5$ and more slowly when higher mole fractions of $Cr(OH)_3$ were used. In general, aqueous Cr concentrations decrease with decreasing Cr contents in the solids, suggesting that $Cr_xFe_{1-x}(OH)_3$ behaves thermodynamically like a solid solution. Activity coefficients for $Cr(OH)_3$ in the solid solutions were calculated from the solubility data and are given by the equation $\log \lambda_{Cr(OH)_3} = -1.60 + 0.28(1-x)^2 - 1.79(1-x)^3$ for $0.01 \leq x \leq 0.69$. Aqueous Fe activities were generally too low for reliable measurement; therefore, the corresponding activity coefficients for $Fe(OH)_3$ [$\log \lambda_{Fe(OH)_3} = -2.26x^2 + 1.39x^3$] were calculated by a Gibbs-Duhem equation. A general relationship [$\log (CrOH^{2+}) = -2pH + 4.18 + 0.28(1-x)^2 - 1.79(1-x)^3 + \log x$] developed from these data can be used to calculate Cr concentrations in solutions between pH 2 and 6 that are in equilibrium with Cr-bearing ferric hydroxides with known Cr content.

Introduction

To predict maximum elemental concentrations of Cr in groundwaters, thermochemical data are needed for Cr-containing solids that are either initially present or potentially occurring in chemical wastes and in permeable rocks. However, thermochemical data are generally not known for Cr-bearing solids that can form in low-temperature, aqueous environments.

Chromium-bearing solids that can limit groundwater Cr concentrations must have low solubilities and rapid precipitation kinetics. The solid phases that are most likely to control Cr concentrations in surface enviroments are $Cr(OH)_3$ and Cr(III) coprecipitated with Fe oxides.[1] Rai et al.[2] have shown that the precipitation/dissolution kinetics of $Cr(OH)_3$ are rapid and that the solubility between pH 6 and pH 10.5 is very low. However, apart from the observed close association of Cr with iron compounds,[3-5] no quantitative data yet exist for Cr(III) coprecipitated with Fe oxides.

Because Cr^{3+} and Fe^{3+} have like charge and similar ionic radii (0.63 Å and 0.64 Å, respectively[6]), amorphous hydroxide precipitates of these elements at room temperature may behave thermodynamically like true solid solutions. If a solid solution represented by the formula $Cr_xFe_{1-x}(OH)_3$ does form readily at room temperature and has lower solubility than $Cr(OH)_3$, its presence would play an extremely important role in controlling Cr(III) concentrations in groundwaters. The results presented here show that (1) $Cr_xFe_{1-x}(OH)_3$ forms readily at room tem-

† Present address: Department of Chemistry, University of Pennsylvania, Philadelphia, PA 19104-6323.

(1) Rai, D.; Zachara, J. M.; Schwab, A. P.; Schmidt, R. L.; Girvin, D. C.; Rogers, J. E. "Chemical Attenuation Rates, Coefficients, and Constants in Leachate Migration"; Report EA-3356; Electric Power Research Institute: Palo Alto, CA, 1984; Vol. 1.
(2) Rai, D.; Sass, B. M.; Moore, D. A. *Inorg. Chem.* **1987**, *26*, 345.
(3) Nakayama, E.; Kuwamoto, T.; Tsurubo, S; Fuginaga, T. *Anal. Chim. Acta* **1981**, *131*, 247.
(4) Cranston, R. E.; Murray, J. W. *Anal. Chim. Acta* **1978**, *99*, 275.
(5) Shiraki, K. In *Handbook of Geochemistry*; Wedepohl, K. H., Ed.; Springer-Verlag: Berlin, 1978; Vol. II/3, Part G.
(6) Weast, R. C., Ed. *Handbook of Chemistry and Physics*; The Chemical Rubber Co.: Cleveland, OH, 1984.

0020-1669/87/1326-2228$01.50/0